Charge storage in Co nanoclusters embedded in SiO_2 by scanning force microscopy

D. M. Schaadt and E. T. Yu[a)]
Department of Electrical and Computer Engineering, University of California at San Diego, La Jolla, California 92093

S. Sankar and A. E. Berkowitz
Center for Magnetic Recording Research, University of California at San Diego, La Jolla, California 92093

(Received 8 September 1998; accepted for publication 9 November 1998)

Scanning force microscopy was used to study localized charge deposition and subsequent transport in Co nanoclusters embedded in SiO_2 deposited on an *n*-type Si substrate. Co nanoclusters were charged by applying a bias voltage pulse between tip and sample, and electrostatic force microscopy was used to image charged areas, to determine quantitatively the amount of stored charge, and to characterize the discharging process. Charge was deposited controllably and reproducibly within areas ~20–50 nm in radius, and an exponential decay in the peak charge density was observed. Longer decay times were measured for positive than for negative charge; this is interpreted as a consequence of the Coulomb-blockade energy associated with single-electron charging of the Co nanoclusters. © *1999 American Institute of Physics.* [S0003-6951(99)01803-3]

Discontinuous metal/insulator multilayers exhibit a variety of properties of importance for potential applications in magnetic recording, the most notable being negative magnetoresistance due to spin-polarized tunneling between the metal particles and saturation of this magnetoresistance at low magnetic fields.[1,2] The transport properties of these materials are of key importance for sensor applications, but are usually observed globally due to the large electrode area typically employed. However, the scanning probe microscope[3] (SPM) provides a method to characterize these properties locally: previous studies have demonstrated local charging of insulator films[4,5] and nitride-oxide-semiconductor structures,[6,7] and imaging of the deposited charge by scanning probe techniques.

In this letter, we describe local charging by a conductive scanning probe tip of a thin film consisting of Co nanoclusters embedded in insulating SiO_2, deposited on a Si substrate. Electrostatic force microscopy (EFM) was used to characterize the local charge density in the Co layer, and the carrier transport both within the discontinuous Co layer and between the Co layer and the Si substrate. Controlled deposition of small numbers of electrons by a proximal probe is demonstrated and quantified; charge decay time is characterized as a function of carrier type and layer structure, and evidence of Coulomb-blockade effects is observed at room temperature in the dynamics of charge decay for positively and negatively charged nanoclusters.

Samples were prepared by alternating sputtering from two separate targets onto an *n*-type Si (100) substrate covered with a native oxide layer (~2.5 nm in thickness). The Co was direct current (dc) sputtered and the SiO_2 was radio frequency (rf) sputtered. Deposition was performed at room temperature with 2 mTorr Ar pressure. The base pressure in the sputtering system was $\sim 10^{-7}$ Torr. The nominal deposited film structure is SiO_2(3 nm)/Co(1.4 nm)/ SiO_2(3 nm), as determined from the deposition rates (0.9–1.3 nm/min for the Co and 2.0–3.0 nm/min for the SiO_2), calibrated by low-angle x-ray reflection. Transmission electron microscopy (TEM) studies have shown that, when deposited on SiO_2, the Co layer is discontinuous with formation of Co nanoclusters,[8,9] as depicted in Fig. 1.

Scanning probe studies were performed at room temperature under ambient conditions using a Digital Instruments MultiMode™ Scanning Probe Microscope[10] with a heavily doped p^+-Si tip. Sample charging was achieved during TappingMode™ operation[9] by holding the tip at the center of the scan area for 10 s with a bias voltage applied to the tip and the sample grounded, as shown in Fig. 1, causing carriers to tunnel between the tip and the Co layer. Little variation in sample charging was observed for charging times ranging from 5 to 30 s. EFM was used to image charged regions and to estimate the total stored charge. A series of EFM images obtained before and after charging at different bias voltages is shown in Fig. 2. Charged areas are observed as peaks or dips in the EFM images, depending on the relative sign of the charging and imaging voltages. No

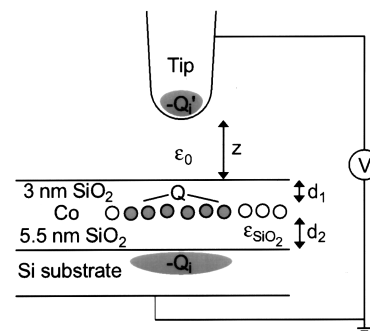

FIG. 1. Schematic diagram of the SiO_2/Co/SiO_2/Si sample structure, probe tip, and voltage bias connections. The charge Q deposited in the Co layer induces image charges $-Q_i$ in the Si substrate and $-Q_i'$ in the tip.

a)Electronic mail: ety@ece.ucsd.edu

 © 1999 American Institute of Physics

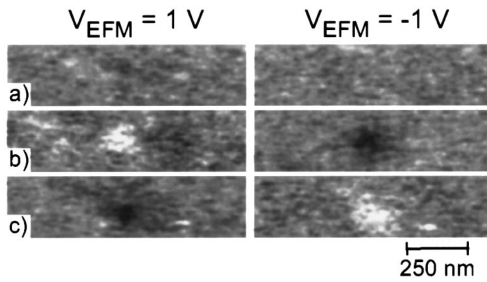

FIG. 2. EFM images obtained with positive and negative bias (a) before charging, and after charging with (b) 12 and (c) −12 V. Charged areas are observed as bright and dark spots for EFM bias and charging voltages of the same and opposite sign, respectively.

charging was observed in a control sample in which no Co layer was present.

The contrast observed in the EFM image may be used to calculate the total stored charge Q. Specifically, the shift Δf in the resonant frequency of the cantilever is related to the force gradient $F' \equiv dF/dz$ by expression $\Delta f = -f_0 f'(z_0)/(2k)$,[11] where $z_0 = 20$ nm is the lift height during EFM imaging, $f_0 = 232$ kHz the cantilever resonant frequency, and k the cantilever spring constant, which was estimated from the lever geometry to be 90 ± 10 N/m. The force $F(z)$ arises from Coulomb interactions of the stored charge, its image charges in the tip and Si substrate, and the induced charges due to the voltage V_{EFM} applied during imaging. From an electrostatic analysis of the tip-sample system modeled using a simple parallel-plate geometry, the force is found to be given by

$$F(z) = \frac{1}{(z + (d_1 + d_2)/\epsilon_{\mathrm{SiO}_2})^2} \times \left(-\frac{d_2^2 Q^2}{{\epsilon_{\mathrm{SiO}_2}}^2 \epsilon_0 A} + \frac{2 d_2 Q V_{\mathrm{EFM}}}{\epsilon_{\mathrm{SiO}_2}} + \frac{\epsilon_0 A V_{\mathrm{EFM}}^2}{2} \right), \quad (1)$$

where d_1 and d_2 are the thicknesses of the top and bottom oxide layer, respectively, $\epsilon_{\mathrm{SiO}_2}$ the relative dielectric constant of SiO_2, z the tip-sample separation, and A the area of the charged region. Model calculations suggest that the first term in the bracket in Eq. (1) is small, a conclusion supported by measurements with $V_{\mathrm{EFM}} = 0$ V showing no contrast difference between charged and uncharged regions. The third term in the bracket is independent of the stored charge and yields a constant background frequency shift at all points in the EFM image. Thus, the final contrast observed is proportional to the stored charge Q and to V_{EFM}. Using the value for f_0, k, z, d_1, and d_2 given above, the total charge Q is then given by $Q = 18 \pm 2\ \mathrm{eV\,Hz}\, V_{\mathrm{EFM}} \Delta f$.

Figure 3 shows the charge deposited in the Co layer, calculated from the contrast measured in EFM images in the manner described above, as a function of the charging voltage V_{ch}. A positive bias applied to the tip results in a positive charge in the Co layer, from which we conclude that charge transfer occurs between the tip and the Co layer, rather than from the Si substrate. The measured dependence of deposited charge on V_{ch}, shown in Fig. 3, yields a value for the tip-sample capacitance $C_m = 1.76 \pm 0.02$ eV. The charged area A may then be deduced from an analysis of the

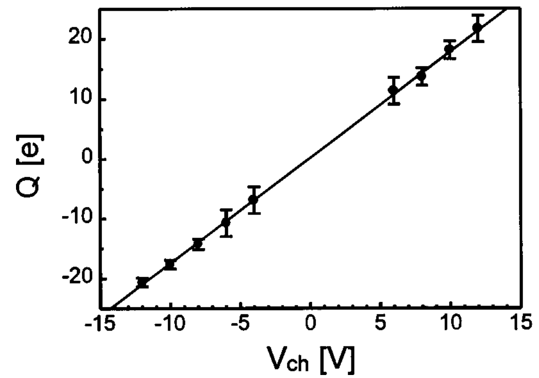

FIG. 3. Initially deposited charge as a function of charging voltage. The line represents a linear fit $Q = C_m V_{\mathrm{ch}}$ with $C_m = 1.76 \pm 0.02$ eV.

tip-induced charging process. Charging occurs while the tip is oscillating, with an average capacitance given by

$$\bar{c} = \frac{\epsilon_0 A}{2B} \int_0^{2B} \frac{1}{z + (d_1 + d_2)/\epsilon_{\mathrm{SiO}_2}} dz, \quad (2)$$

where $B = 90$ nm is the measured amplitude of the tip oscillation. By requiring that $\bar{C} = C_m$ we deduce a value for the charged area A of $\sim 1300\ \mathrm{nm}^2$, corresponding to a disk with a radius of ~ 20 nm, which is in reasonable agreement of the radius of the charged region of 70–100 nm in the EFM images minus the tip radius of 10–20 nm. TEM images of similar samples show that approximately 20–40 Co nanoclusters are present within an area of the size.[8,9] Thus, charging at ± 12 V deposits or removes approximately one electron per Co nanocluster.

Figure 4 shows EFM images of a charged region 30, 150, and 330 s after charging. The charged region can be seen to increase slightly in area over time, with the contrast between charged and uncharged regions decreasing strongly. These observations indicate that most of the stored charge tunnels into the Si substrate, with some carrier transport also occurring between Co nanoclusters. This conclusion is supported by measurements performed on structures with a thick SiO_2 layer beneath the Co layer, in which much longer charge decay times were observed. Figure 5 shows the decay in charge for regions charged at 12 and −12 V. The charge

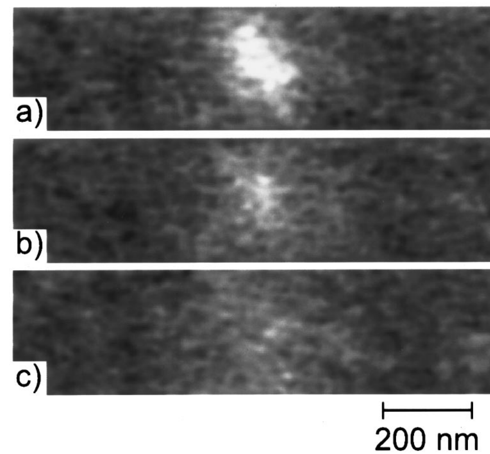

FIG. 4. EFM images (a) 30, (b) 150, and (c) 330 s after charging at 12 V, showing a gradual decrease in peak charge density and slight increase in area.

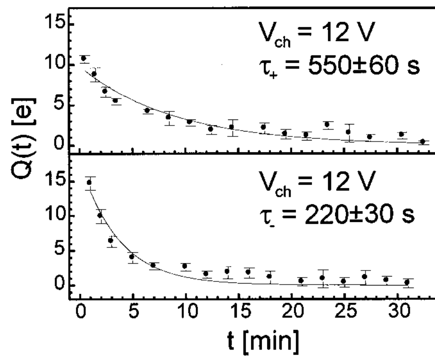

FIG. 5. Decay of stored charge for $V_{ch}=12$ (top) and -12 V (bottom). Symbols are experimental data, and the solid lines are fitted curves with functional form $Q(t)=Q_0 \exp(-t/\tau_\pm)$.

decay appears exponential in both cases, but with different decay times τ_+ and τ_- for positive and negative stored charge, respectively.

We interpret the difference in the decay times for positive and negative charging as a consequence of the Coulomb blockade energy for charging of the Co nanoclusters. To tunnel from a Co nanocluster with a single negative charge into the Si substrate, an electron must overcome a potential barrier $\phi_1=\phi_{Co}-e\chi_{SiO_2}-E_0$ where ϕ_{Co} is the Co work function, χ_{SiO_2} the SiO_2 electron affinity, and $E_0=e^2/(2C_{Co})$ the single-electron charging energy[12] of a Co nanocluster with capacitance C_{Co}. To escape from a nanocluster with a single positive charge, a hole must overcome a potential barrier $\phi_2=\phi_{Co}-e\chi_{SiO_2}+E_0$. Since the tunneling probability T varies with barrier height ϕ and barrier thickness d as $T \sim \exp(-2d\sqrt{2me\phi}/\hbar)$, the relation between the decay times is given approximately by

$$\frac{\tau_+}{\tau_-} \approx e^{\frac{2d_2\sqrt{2me}}{\hbar}(\sqrt{\phi_2}-\sqrt{\phi_1})}, \tag{3}$$

where m is the electron mass and d_2 the lower SiO_2 layer thickness. Solving Eq. (3) for the charging energy and using the measured values for τ_+ and τ_-, we obtain $E_0=33\pm6$ meV. TEM images of similar structures show spherical Co particles $\sim$1.5 nm in radius in chain-like arrangements with typical lengths of 3–6 particles.[8,9] The charging energy of such nanoclusters is approximately 31 ± 10 meV, which is in very good agreement with the value estimated from measured decay times. Measurements on samples with larger Co clusters show that the difference between τ_+ and τ_- decreases as the Co cluster size increases, as expected since E_0, and therefore $\phi_2-\phi_1$, decrease with increasing cluster size.

In summary, we have used scanning probe techniques to demonstrate and characterize local charge deposition and transport in Co nanoclusters embedded in an insulating SiO_2 matrix. Positive and negative charge can be deposited controllably and reproducibly in such nanoclusters, typically in quantities of $\sim$5–20 electrons within areas 30–50 nm in radius. The charge decays over several minutes, with the decay time for positively charged nanoclusters being substantially larger than that for negatively charged nanoclusters. This difference is interpreted as a consequence of the Coulomb blockade energy associated with single-electron charging of Co nanoclusters.

Part of this work was supported by ONR (Grant No. N00014-95-1-0996) and NSF (Award Nos. ECS95-01469 and DMR 9400439). E.T.Y. would like to acknowledge financial support from the Alfred P. Sloan Foundation.

[1] S. Sankar, B. Dieny, and A. E. Berkowitz, J. Appl. Phys. **81**, 5512 (1997).
[2] K. R. Coffey, T. L. Hylton, M. A. Parker, and J. K. Howard, Scr. Metall. Mater. **33**, 1593 (1995).
[3] G. Binnig, C. F. Quate, and C. Gerber, Phys. Rev. Lett. **56**, 930 (1986).
[4] B. D. Terris, J. E. Stern, D. Rugar, and H. J. Mamin, Phys. Rev. Lett. **63**, 2669 (1989).
[5] B. D. Terris, J. E. Stern, D. Rugar, and H. J. Mamin, J. Vac. Sci. Technol. A **8**, 374 (1990).
[6] R. C. Barrett and C. F. Quate, J. Appl. Phys. **70**, 2725 (1991).
[7] M. Dreyer and R. Wiesendanger, Appl. Phys. A: Solids Surf. **61**, 357 (1995).
[8] S. Sankar, D. J. Smith, and A. E. Berkowitz, Appl. Phys. Lett. **73**, 535 (1998).
[9] B. Dieny, S. Sankar, M. R. McCartney, D. J. Smith, and A. E. Berkowitz, J. Magn. Magn. Mater. **185**, 283 (1998).
[10] MultiMode and TappingMode are trademarks of Digital Instruments, Santa Barbara, CA.
[11] Y. Martin, C. C. Williams, and H. K. Wickramasinghe, J. Appl. Phys. **61**, 4723 (1987).
[12] P. Sheng and B. Abeles, Phys. Rev. Lett. **28**, 34 (1972).